

Prevention and Control Analysis of Rockburst Using Drilling Pressure Relief in Surrounding Rock Mass of Deep Tunnel

Zihui Zhu¹, Qirui Wang^{2,*}, Jiaqi Guo¹, Yongsheng He² and Feiyue Sun³

¹School of Civil Engineering, Henan Polytechnic University, Jiaozuo 454003, China

²International Institute of Defense Engineering, AMS, PLA, Luoyang, 471023, China

³School of Emergency Management, Henan Polytechnic University, Jiaozuo 454003, China

Received 2 May 2023; Accepted 24 August 2023

Abstract

With the increase of engineering construction scale and buried depth, the frequency and intensity of rockburst are increasing, which severely affects the safety construction of deep tunnels. Drilling pressure relief has become a commonly used method for actively preventing rockburst. Based on 3D discrete element software, a numerical study was carried out on rockburst prevention and control in deep tunnels by drilling pressure relief. Combined with the multi-parameter rockburst index considering the rockburst key factors and the stress state of the rock unit, the drilling effect on rockburst prevention and control was evaluated. Results show that the fracture zone of large-scale pressure relief is generated along the drilling position distribution after drilling. The stress concentration degree and energy storage level inside the fracture zone are significantly reduced, and the stress concentration and energy accumulation area are transferred to the deep rock mass. Compared with the drilling diameter D , the drilling length L has a more obvious influence on the surrounding rock. Considering the rockburst key factors and the tensile and compressive stress of the rock unit, the proposed rockburst index REC (rockburst energy criterion) can accurately evaluate rockburst occurrence location and intensity level, and comprehensively reflect the drilling effect on the rock mass rockburst tendency. The conclusions obtained in this study provide significant references to evaluate the drilling effect on rockburst prevention and control in deep tunnels.

Keywords: Deep tunnel, Rockburst, Drilling pressure relief, Drilling parameter, Numerical simulation

1. Introduction

With the in-depth implementation of national strategies such as “Chinese Western Development” and “One Belt One Way”, the development and utilization of underground resources, and the deepening of underground engineering construction, the underground tunnels such as hydropower traffic tunnels and mine roadways have gradually advanced to the deep [1-2]. The geological conditions of the rock mass are more complicated, the ground stress level increases obviously, and disasters such as rockburst occur frequently during the construction process, which greatly threatens the construction safety and equipment life, and seriously hinders the normal development of the construction [3-6]. How to prevent and control the occurrence of rockburst has become one of the engineering problems that cannot be ignored and needs to be solved urgently. So, it is of great engineering significance to carry on a relevant study about rockburst disaster prevention and control to ensure the normal development and safe construction of underground engineering.

Rockburst is one of the most serious geological disasters in the worldwide underground engineering. However, it is difficult to be predicted timely, because it often occurs without obvious precursors. Many experts and scholars have proposed a series of rockburst prevention and control theories and targeted prevention and control measures for

the characteristics and mechanisms of the rockburst development process in recent years, and successfully applied them to engineering practice, such as optimizing excavation schemes, surrounding rock pretreatment and reinforcement support [7-9]. Among them, the drilling pressure relief technology is one of the most effectively used pretreatment methods for surrounding rock to actively control and avoid rockburst occurrence, which plays the role of pressure relief and energy dissipation using drilling in the deep rock mass, to achieve the purpose of rockburst prevention and control [10]. Therefore, it is important to explore the internal mechanism of rockburst prevention and control using the drilling pressure relief technology.

2. State of the art

At present, scholars have carried out deep studies about the mechanism, parameter optimization, and effect evaluation of drilling pressure relief. Guo et al. [11] reviewed the experimental progress of rockburst prevention and control by prefabricated boreholes and high-stress real-time boreholes from both macro and micro aspects, and they described the rationality of drilling pressure relief for rockburst prevention and control. Liu et al. [12] analyzed the variation of borehole numbers on the failure characteristics of sandstone strain-type rockburst. They found that the increase of the drilling number could availability reduce the

*E-mail address: lywqr3061@163.com

ISSN: 1791-2377 © 2023 School of Science, IHU. All rights reserved.

doi:10.25103/jestr.164.13

risk level of rockburst and the fragmentation degree of ejection debris, which had a good rockburst prevention and control effect. Now, the rock mechanics experiment related to drilling pressure relief has been developed rapidly, but it is still limited by the existing system conditions. Most of the experiments are uniaxial compression tests, which cannot fully reflect the whole stress state before and after tunnel excavation and drilling, and the specific evolution characteristics of multi-information inside the surrounding rock before and after drilling cannot be fully visualized.

The numerical simulation method solves the problem that the laboratory test cannot meet [13-18]. Manouchehrian et al. [19-20] studied the feasibility of the slotting pressure relief method in strain-type rockburst control, and they carried out parameter optimization on the pressure relief process of the circular tunnel in numerical simulation. According to the dissipative energy theory, Zhao et al. [21] established a large-diameter borehole model, and they studied the energy transformation of coal under the influence of mining depths and borehole spacings by numerical simulation. Chen et al. [22] combined PFC software to analyze the stress evolution and failure mode of rock mass with different drilling positions and depths. They found that the pressure relief effect was not continuously improved after the drilling depth reached 1500 mm. Zhang et al. [23] simulated the three-dimensional spatial effect of drilling with stress release rate, and they analyzed the effect of multi-drilling parameters on rockburst prevention and control. The above research is of great significance for rockburst prevention and control by drilling pressure relief. However, the above analysis about the evolution characteristics of rock mass information before and after drilling is only carried out from the stress or energy unilaterally, which cannot fully reflect the drilling effect on the surrounding rock, and there are few studies on the effect evaluation of rockburst prevention and control by drilling pressure relief [24-27].

Therefore, based on the secondary development of a 3D discrete element simulation platform, the numerical evaluation and analysis of the drilling effect on rockburst prevention and control in the deep tunnel were carried out, and the visualization of stress, energy, and rockburst tendency characteristics of deep rock mass were analyzed by drilling pressure relief. The influence of drilling length and diameter on the multivariate information evolution characteristics of surrounding rock was compared and analyzed. Considering the key rockburst factors and the overall stress state of the rock unit, the drilling pressure relief effect on rockburst prevention and control was evaluated with a multi-parameter rockburst index. The research results can provide a relevant basis for rockburst prevention and control in deep tunnels.

The rest of this study is organized as follows. Section 3 introduces the mechanism of rockburst prevention and control using drilling pressure relief and the establishment of the numerical model. Section 4 gives the simulation results analysis and discussion, and finally, the conclusions are summarized in Section 5.

3. Methodology

3.1 Mechanism of rockburst prevention and control using drilling pressure relief

The surrounding rock mass in the deep tunnel is mostly completely hard brittle rock under high ground stress

conditions. Due to the influence of step excavation and complex stress environment, the rock mass stress is redistributed after excavation. The tangential stress near the tunnel wall rises rapidly, and the axial stress declines rapidly, showing a single-sided unloading stress state. While the tangential stress reaches the strength of the rock itself, the surrounding rock is prone to instability and failure, which induces multi-frequency and high-strength rockburst disaster. To reduce the rockburst intensity as much as possible, it is necessary to take measures to change the mechanical state of the rock unit, so as to redistribute the rock stress state after excavation, and then reduce and transfer the tangential stress at the tunnel wall.

Drilling pressure relief technology is widely used in underground coal mines, diversion tunnels, and railway/highway tunnels around the world. It is one of the best measures for rockburst prevention and control in deep tunnels. Through the artificial drilling of the high energy storage rock mass with rockburst tendency, the tangential stress amplitude reduces and the energy stored inside the rock mass is released, which is transferred to the deep rock mass, and a large area of fracture zone is formed around the boreholes in the deep rock mass. Considering the elastic characteristics of the rock around the boreholes after drilling, the rock mass will expand and fill the free space, and the radial deformation inside the rock mass will be transformed into tangential deformation [19]. Under the combined action of multiple boreholes, the fracture zones formed are interconnected, and a larger range of pressure relief fracture zones will be formed around the surrounding rock, so that the stress concentration area will shift to the deep rock mass. The rock mass strength inside the fracture zone declined, and the corresponding stress concentration degree was reduced. The theory of drilling pressure relief is shown in Fig. 1.

On the one hand, drilling pressure relief plays a role in stress release and energy dissipation. The fracture zone reduces the stress concentration, energy storage, and bearing capacity of the surrounding rock. On the other hand, it destroys the rock integrity and changes the rock stress state, so as to reduce the possibility of rockburst occurrence. At present, the drilling pressure relief technology is mainly suitable for weak-medium grade rockburst, and the rockburst prevention and control effect is closely related to the drilling direction, depth, diameter, and spacing. Some scholars generally divided the drilling pressure relief methods into two categories: (1) radial pressure relief borehole, which was widely used in the early stage of tunnel excavation and usually applied to the tunnel wall. (2) The advanced pressure relief borehole was vertically applied to the unexcavated high-risk palm face to weaken the rockburst intensity in front of the palm face.

3.2 Establishment of numerical calculation model in deep tunnel

3.2.1 Numerical model and boundary condition

Taking a deep-buried straight wall arched tunnel as an example, based on the Saint-Venant principle, considering the acting range of tunnel excavation, a calculation model of $60 \text{ m} \times 50 \text{ m} \times 20 \text{ m}$ (length \times height \times width) was established. The model's upper boundary and the free surface formed by tunnel excavation were free boundaries. The upper boundary applied a uniform load of 29.623 MPa, and the remaining constraint boundary conditions were normal displacement constraint boundaries. To improve the

accuracy of numerical calculation, the straight wall arched tunnel was designed at the geometric center of the calculation model. Because of the symmetrical structure of the excavation tunnel, only monitoring points were set for the key parts on one side of the tunnel. Fig. 2 is the numerical calculation model.

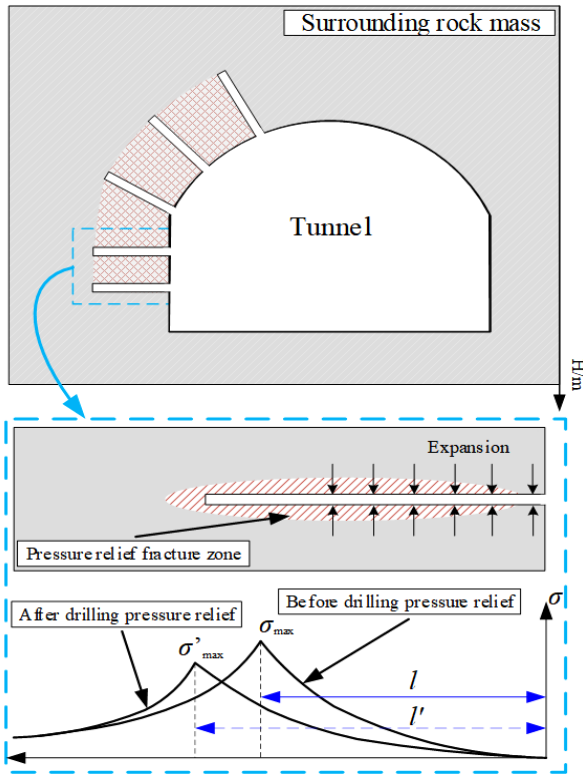


Fig. 1. Schematic of drilling pressure relief [23, 24].

3.2.2 Mechanical parameters of surrounding rock mass

The constitutive relation adopted the M-C (Mohr-Coulomb) yield criterion ($\text{Cons} = 2$) [26]. According to the analysis of engineering geological data, the rock lithology in the rockburst tendency area is mainly composed of granite, and Table 1 shows the mechanical parameters of the surrounding rock mass.

Table 1. Physical and mechanical parameters of surrounding rock mass.

Unit weight ($\text{kN}\cdot\text{m}^{-3}$)	Elasticity modulus (GPa)	Bulk modulus (GPa)	Shear modulus (GPa)	Poisson's ratio	Internal friction angle ($^\circ$)	Cohesion (MPa)	Compressive strength (MPa)	Tensile strength (MPa)
27.03	33.60	20.74	13.66	0.23	48.67	1.48	140	6

3.2.3 Drilling model and scheme design

The establishment of the numerical model needs to fully reflect the excavation sequence of the simulated tunnel, and truly reflect the mechanism and acting effect of drilling pressure relief as much as possible, so as to accurately simulate the mechanical behavior of surrounding rock under different drilling parameters. So, during the simulation process of drilling pressure relief, the equivalent method of establishing a drilling model was used to simulate the drilling pressure relief effect. Taking the center of the arched tunnel above as the center, the radial drilling holes were uniformly applied to the arched tunnel above, and the vertical drilling holes were applied to the tunnel wall on both sides of the tunnel. The drilling arrangement is shown in Fig. 3.

Fig. 4 is the displacement vector diagram of the surrounding rock mass before and after drilling. There is a large displacement around the surrounding rock mass before

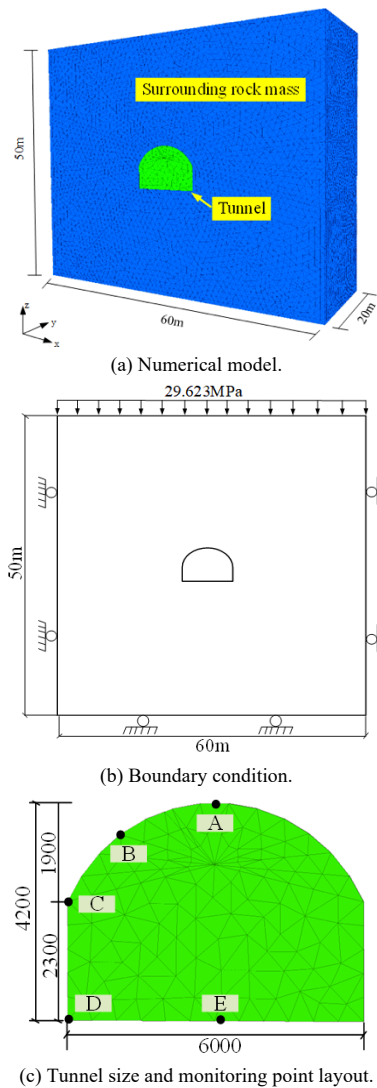


Fig. 2. Numerical calculation model.

drilling, the vectors on both sides and the floor of the tunnel are the most obvious. After drilling, the displacement vector around the surrounding rock is reduced, and the displacement vector appears in a large number inside each borehole. The convergence of the boreholes leads to the radial deformation into the tangential deformation around the boreholes. Therefore, the calculation model established in this study can better reflect the mechanism and effect of drilling pressure relief.

The scheme design can effectively reflect the influence of drilling length and diameter on the multivariate information evolution characteristics of the surrounding rock mass. Table 2 shows the parameter design of the simulated condition, the numerical simulation scheme is designed for 8 conditions. The procedures of numerical simulation are as follows: firstly, the mechanical parameters of rock mass are input and the initial stress balance is calculated, then the tunnel is excavated, and the secondary balance calculation is

carried out. Finally, the drilling boreholes are applied around the tunnel, and the calculation results are output after the calculation model is balanced.

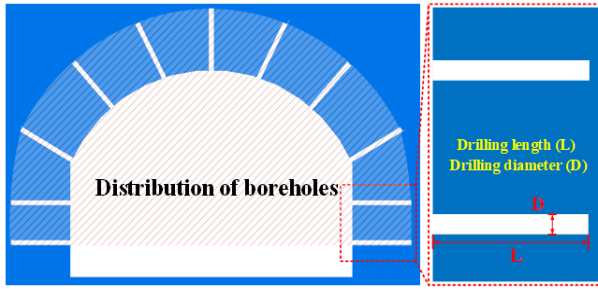
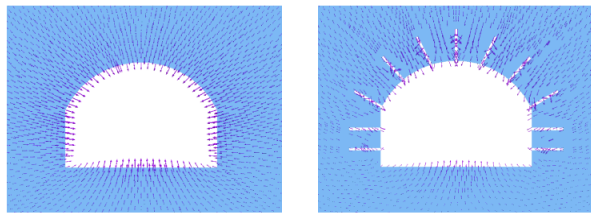


Fig. 3. Model of drilling pressure relief.



(a) Before drilling. (b) After drilling.
 Fig. 4. Distribution of displacement vector.

Table 2. Parameter design of simulated condition.

Condition	Drilling diameter D (mm)	Drilling length L (m)
1	0	0
2	200	1
3	200	1.5
4	200	2
5	200	2.5
6	150	2.5
7	100	2.5
8	50	2.5

4. Result analysis and discussion

4.1 Influence of drilling pressure relief on stress field of surrounding rock mass

The variation of the stress state inside the rock mass under excavation condition is one of the key causes of rockburst occurrence. Considering that the rock unit is in a triaxial stress state before excavation, the FISH language program based on 3DEC is used to calculate the principal stress difference $\Delta\sigma$, that is, the difference of the principal stress between the maximum σ_1 and the minimum σ_3 ($\Delta\sigma = \sigma_1 - \sigma_3$), which can better reflect the local stress concentration. Fig. 5 is the principal stress difference $\Delta\sigma$ distribution of the surrounding rock mass under different drilling parameters.

From Fig. 5, the value of $\Delta\sigma$ during the excavation stage is mainly concentrated near the vault and arch foot on both sides of the tunnel, the maximum value of $\Delta\sigma$ can reach 106.37 MPa. The $\Delta\sigma$ distribution is obviously different before and after drilling. After drilling, a large-scale pressure relief fracture zone formed around the surrounding rock mass along the drilling borehole distribution position, and the $\Delta\sigma$ inside the fracture zone was significantly reduced. In Fig. 5 (b-e), the acting area of the fracture zone gradually increases with the drilling length L . In Fig. 5 (e-h), when L is constant, the stress-weakening effect of the surrounding rock mass is not obvious when D is 50 mm. However, when D is between 100 ~ 200 mm, the acting area of the fracture zone is almost unchanged.

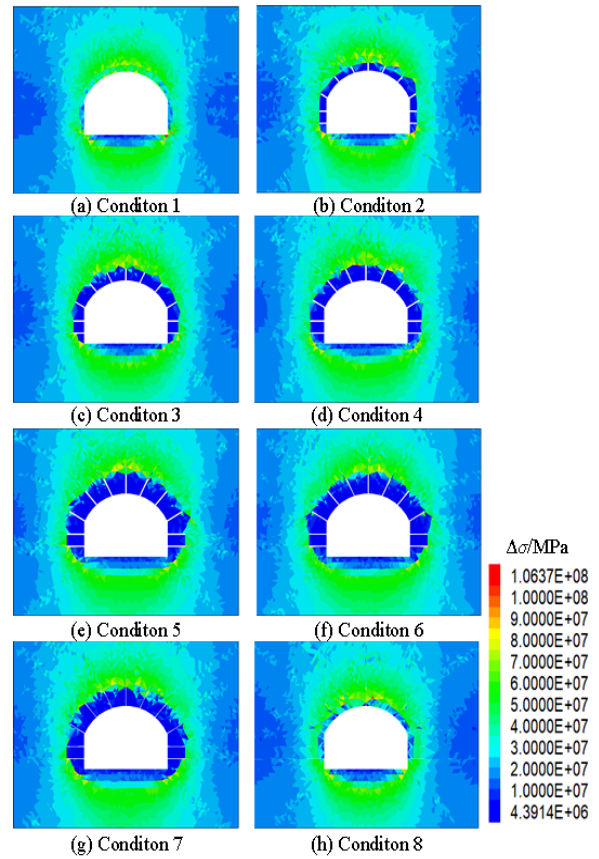


Fig. 5. Distribution of principal stress difference $\Delta\sigma$.

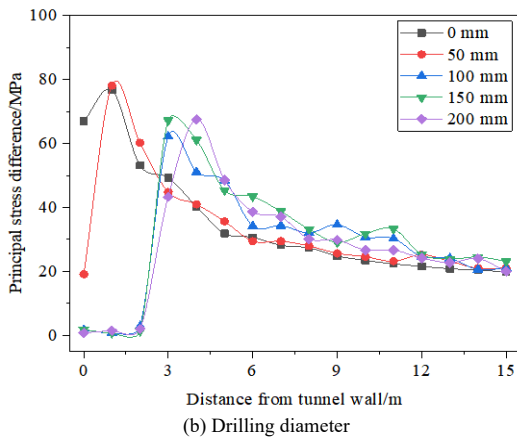
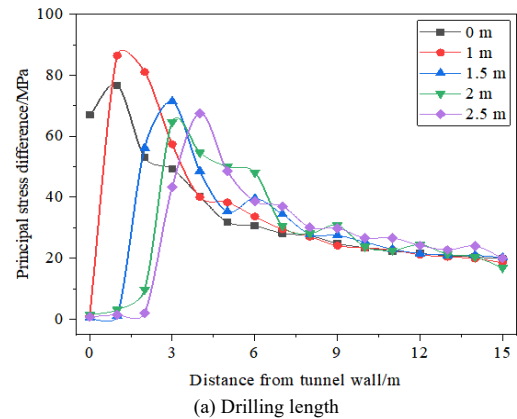


Fig. 6. Influence of drilling pressure relief on principal stress difference distribution.

Considering the approximate stress state of each rock unit around the tunnel, taking monitoring point A as an example, the influence of drilling length and diameter on the

$\Delta\sigma$ distribution is further analyzed. As can be seen in Fig. 6, where the x-axis represents the distance from the tunnel wall. The distribution characteristics of $\Delta\sigma$ under different drilling parameters are approximately the same, showing the characteristics of asymmetric inverted V-shaped variation. The value of $\Delta\sigma$ increases with the distance from the tunnel wall, which quickly reaches the peak in the pressure relief zone and then enters the elastic zone and gradually decreases. Finally, it tends to stabilize and enters the original rock stress area. The variation trend is nearly consistent with the previous research results [27]. From Fig. 6(a), the value of $\Delta\sigma$ near the tunnel vault after excavation is about 66.91 MPa, and the stress concentration area is mainly distributed near 1m from the tunnel wall. When L is 1 m, the value of $\Delta\sigma$ inside the rock mass wall decreases rapidly, and the stress concentration area is still distributed near 1m from the tunnel wall, and its peak value is 112.77 % of the peak value after excavation. As L increases, the acting area of the fracture zone gradually increases and shifts to the deep rock mass. When L is 2.5 m, the principal stress difference within about 2 m from the tunnel wall is only between 0.78 ~ 2.04 MPa, and the stress concentration area is about 4 m from the tunnel wall. The peak value is about 88 % of the peak value after excavation. When D is 50 mm, the value of $\Delta\sigma$ near the tunnel wall is about 20 MPa, and the peak value and position of $\Delta\sigma$ are almost unchanged. When D is between 100 ~ 200 mm, the principal stress difference decreases rapidly within 2 m from the tunnel wall, and the stress concentration area is distributed in the vicinity of about 3 ~ 4 m from the tunnel wall. When D is 200 mm, the area of stress concentration is farther away from the tunnel wall than D of 150 mm.

4.2 Influence of drilling pressure relief on the energy distribution of surrounding rock mass

Based on the 3DEC built-in FISH language program, the calculation of the releasable elastic strain energy density (U^e) is programmed, and the calculation equation of the strain energy is shown in Eq. (1) [28]. The U^e distribution characteristics of the surrounding rock mass are shown in Fig. 7.

$$U^e \approx \frac{1}{2E_0} [\sigma_1^2 + \sigma_2^2 + \sigma_3^2 - 2\nu(\sigma_1\sigma_2 + \sigma_2\sigma_3 + \sigma_1\sigma_3)] \quad (1)$$

where σ_1 , σ_2 , and σ_3 are the principal stress of maximum, intermediate, and minimum of the surrounding rock mass. To adapt to engineering practice, E_0 and ν are the initial elastic modulus and initial Poisson's ratio, respectively.

As can be seen in Fig. 7, the energy distribution of the surrounding rock mass is approximately consistent with the stress field characteristics. The maximum value of U^e is distributed at the vault and the arch foot on both sides of the tunnel when there is no drilling. After drilling, the high energy storage inside the rock mass within the fracture zone is rapidly released and transferred, and the peak energy is transferred to the deep rock mass. The weakening effect of the drilling length on the energy distribution inside the rock mass is more obvious than that of the drilling diameter.

Fig. 8 shows the drilling effect on the U^e distribution of the surrounding rock mass. Taking the monitoring point A as an example, in Fig. 8(a), the peak value of U^e near the tunnel wall after excavation is about 0.079 MJ/m³, and the peak energy is mainly concentrated near 1m from the tunnel wall. The high energy accumulation stored inside the rock mass will compensate for the other surrounding rocks, and the tunnel vault is prone to rockburst. When L is 1 m, the energy stored inside the rock mass at the tunnel wall is rapidly

released, transferred to the deep rock mass, and accumulated about 1m from the tunnel wall, and its energy is about 1.45 times of the peak energy without drilling. As L increases, the energy accumulation area is further transferred to the deep rock mass. When L reaches 2.5 m, the value of U^e inside the rock mass is almost 0 within 2 m from the tunnel wall, and the peak of U^e is about 4 m from the tunnel wall. The peak value is about 85% of the peak energy after excavation. When D is 50 mm, the value of U^e near the tunnel wall is about 0.0085 MJ/m³, with a decrease of 89.24%, and the peak energy position is almost unchanged, with an increase of about 25%. When D is between 100 ~ 200 mm, the value of U^e is almost 0 within about 2 m from the tunnel wall, indicating that the fracture zone generated by drilling pressure relief makes the energy inside the rock mass completely released. When D is 100 mm and 150 mm, the peak energy is mainly concentrated about 3m from the tunnel wall, and the peak energy with D of 200 mm is about 4 m from the tunnel wall, and the peak energy is slightly reduced.

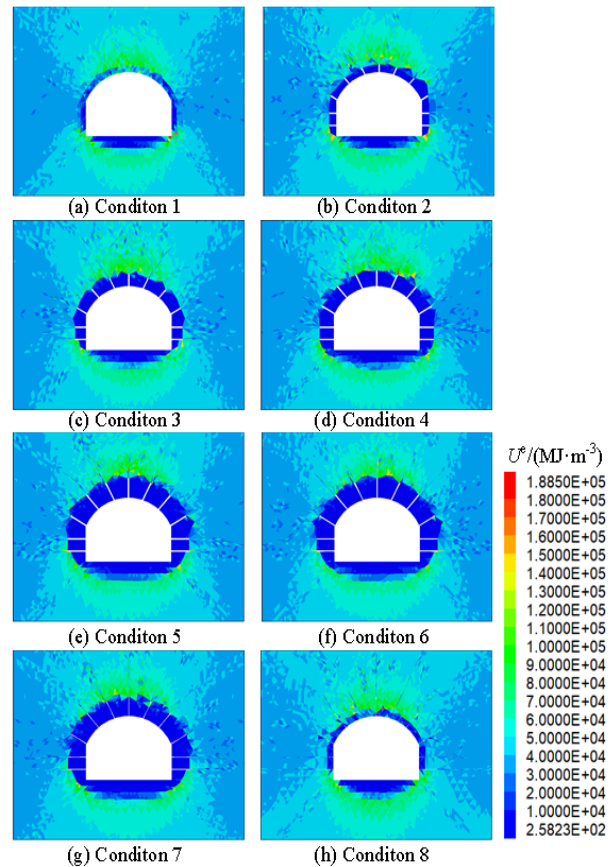
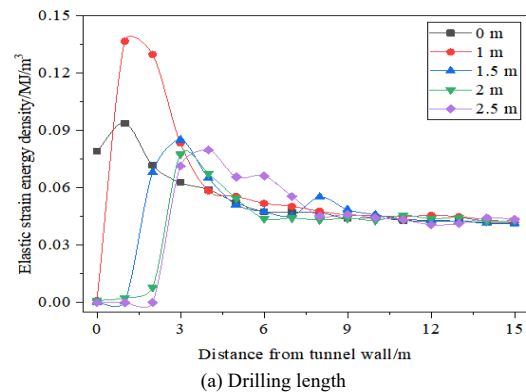


Fig. 7. Distribution of elastic strain energy density U^e .



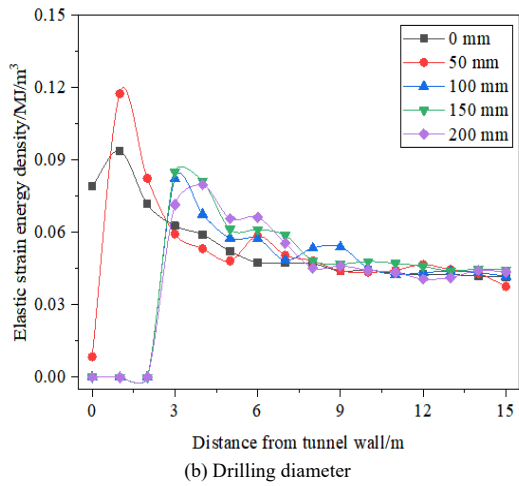


Fig. 8. Influence of drilling pressure relief on elastic strain energy density distribution.

4.3 Influence of drilling pressure relief on rockburst tendency of surrounding rock mass

Rockburst tendency is the key basis for evaluating on rockburst disaster in the deep rock mass. To determine the intensity level and occurrence location of rockburst before and after drilling in the deep tunnel, the influence of drilling pressure relief on rockburst tendency is further analyzed. This section fully considers the key factors affecting

rockburst, namely mechanical, brittleness, integrity, and energy storage factors. Based on the energy principle, the two stress states of tension and compression of rock mass units before and after excavation are fully considered, a multi-parameter rockburst tendency index *REC* (rockburst energy criterion) is proposed [29], as shown in Eq. (2):

$$REC = K_v \left(\frac{\sigma_\theta}{\sigma_c} \frac{\sigma_c}{\sigma_t} \right) \frac{U^e}{U_0} = K_v \frac{\sigma_\theta}{\sigma_t} \frac{U^e}{U_0} \quad (2)$$

where K_v , σ_θ/σ_c , σ_c/σ_t , and U^e/U_0 represent the rock integrity factor, mechanical factor, brittleness factor, and energy storage factor, respectively. σ_θ , σ_c , σ_t are tangential stress, compressive and tensile strength of rock mass, respectively. U_0 is the density of ultimate elastic strain energy. The intensity classification of *REC* is shown in Table 3.

The 3D discrete element simulation is secondary developed through the preparation of FISH language, and the analysis of rockburst tendency is carried out with *REC*. The intensity level and location of the rockburst inside the surrounding rock mass are predicted and evaluated, and the drilling effect on rockburst prevention and control is compared and analyzed. Combined with Eq. (2), Fig. 9 shows the *REC* distribution of the surrounding rock mass under different drilling conditions.

Table 3. Intensity classification of *REC* [23].

Rockburst index	Rockburst grade			
	No	Weak	Moderate	Intense
<i>REC</i>	<0.40	0.40 ~ 1.00	1.00 ~ 5.00	>5.00

As can be seen in Fig. 9, according to the division of *REC* boundary values, the maximum value of *REC* inside the vault and the arch foot on both sides of the tunnel after excavation reaches 5.26, which is a rockburst tendency area, the rockburst grade belongs to intense. The tunnel floor also has a slight rockburst tendency, which the grade is weak. By observing the rockburst tendency of the surrounding rock after drilling, it is found that drilling pressure relief around the surrounding rock can effectively reduce the risk degree of rockburst. As L increases, the area of the fracture zone increases continuously, and the maximum value of *REC* gradually shifts to the deep rock mass. The fracture zone generated by drilling can effectively reduce the rockburst tendency near the tunnel wall.

When L is 2 m, the fracture zone around the drilling bores position is connected with the tunnel floor, and the rockburst tendency of the arch foot on both sides of the tunnel begins to weaken obviously. When L is 2.5 m, there is a certain rockburst tendency only at the tunnel floor, and the peak value of *REC* is almost concentrated at the end of the boreholes, indicating that the end of the boreholes is significantly unstable. When D is 50 ~ 200 mm, the rockburst tendency is almost only in the tunnel floor. Therefore, it is necessary to prevent or avoid rockburst on the tunnel floor after drilling. After drilling, high pressure water or high strength concrete should be sprayed on the surface and inside the boreholes of the deep tunnel in time.

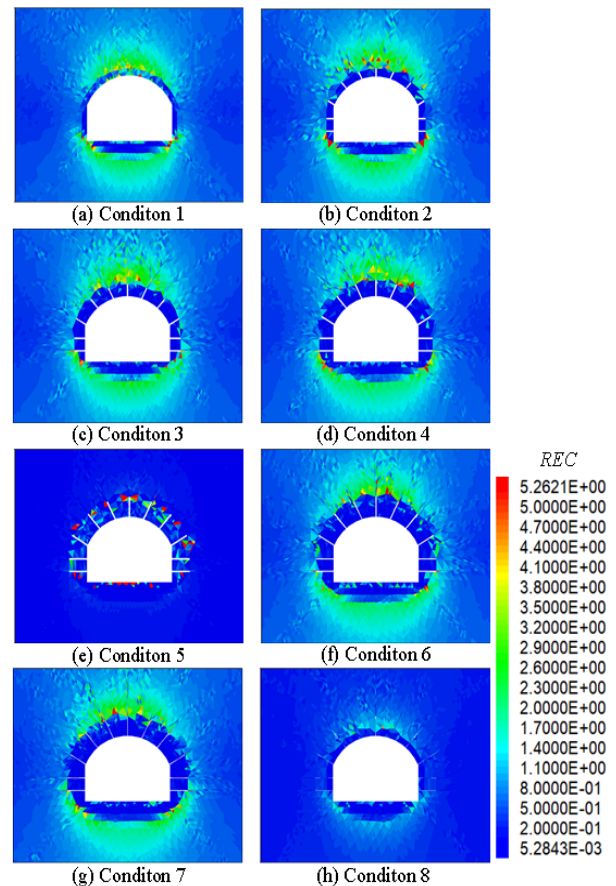


Fig. 9. Distribution of rockburst index *REC*.

Considering the variation trend of $\Delta\sigma$ and U^e can indirectly reflect the brittle failure degree of surrounding rock mass, the above two indexes can be compared and analyzed for the effect of drilling pressure relief, further verifying the rationality of the multi-parameter rockburst index. Taking the optimal drilling parameters as an example ($L=2.5$ m, $D=200$ mm), Fig. 10 is the distribution characteristics of $\Delta\sigma$, U^e , and REC before and after drilling pressure relief at each monitoring point around the surrounding rock. From Fig. 10, after the tunnel excavation, the vault, arch foot, and floor of the tunnel have a medium rockburst tendency, while the arch shoulder position has a weak rockburst tendency, and there is nearly no rockburst at the tunnel haunch.

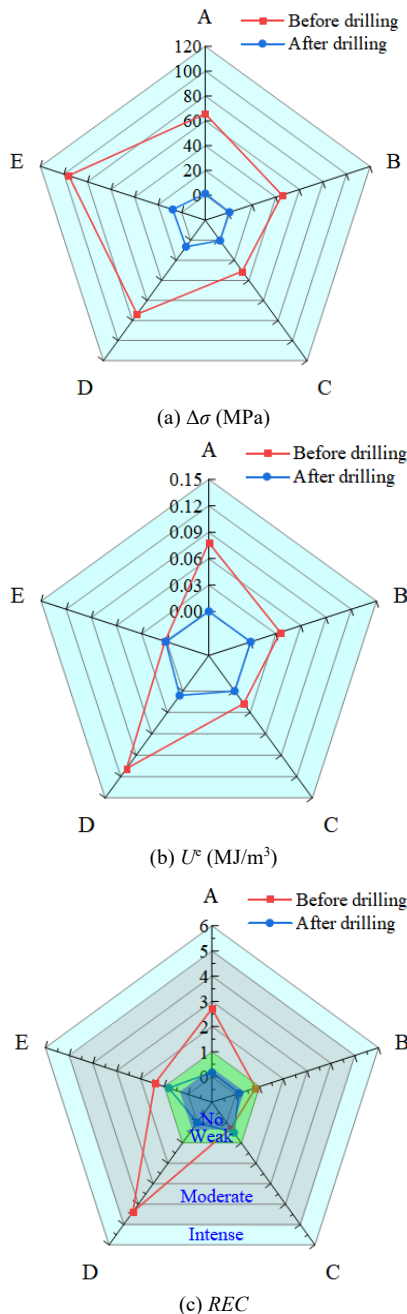


Fig. 10. Multivariate information characteristics at monitoring points before and after drilling.

After drilling, the values of $\Delta\sigma$, U^e , and REC of the surrounding rock mass all decrease rapidly. Only the tunnel floor has a weak rockburst tendency, and no rockburst

occurs in the other monitoring parts. The characteristics of REC , $\Delta\sigma$, and U^e at each monitoring point before and after drilling pressure relief are approximately consistent, indicating that REC can better reflect the stress concentration degree and energy accumulation level of rock units after engineering excavation and drilling pressure relief. It is reasonable and feasible to select REC as the evaluation standard of rockburst prevention and control using drilling pressure relief, and its accuracy needs to be further verified by engineering practice.

5. Conclusions

Based on the secondary development of 3D discrete element numerical simulation, the influences of drilling length and diameter on the multivariate information evolution characteristics of surrounding rock mass were analyzed for rockburst area in a deep tunnel. Combined with the multi-parameter rockburst tendency index REC (rock mass energy criterion), the effect of drilling pressure relief on rockburst prevention and control was evaluated. The following conclusions were drawn.

(1) Drilling pressure relief has a significantly weakening effect on the rock mass multivariate information evolution characteristics in deep tunnels. After excavation, the stress was mainly concentrated near the tunnel wall, where the rock mass is a high energy storage rock. After drilling, a large-scale pressure relief fracture zone forms along the drilling distribution position around the rock mass. The stress concentration and energy storage level inside the fracture zone are significantly reduced, and the stress and energy accumulation area are transferred to the deep rock mass. The drilling convergence leads to the radial deformation into the tangential deformation inside the boreholes of the tunnel.

(2) Compared with the drilling diameter, the drilling length has a more obvious influence on the multivariate information evolution characteristics of the surrounding rock. As drilling length increases, the acting area of the pressure relief fracture zone increases, which the peak values of stress and energy to decrease and gradually transfer to the deep rock mass. As the drilling diameter increases, the acting area of the pressure relief fracture zone is almost unchanged, and the peak value and distribution position of stress and energy do not change significantly. When the drilling length or diameter is small, the peak values of stress and energy inside the rock mass do not decrease but increase, which will further induce a rockburst.

(3) Considering the rockburst key factors and the tensile and compressive stress states of the rock mass units, the proposed multi-parameter rockburst index REC can accurately evaluate the drilling effect on the rockburst tendency of the surrounding rock. After drilling, the peak value of REC gradually shifts to the deep rock mass, and the fracture zone generated using the drilling effectively reduces the rockburst tendency induced by engineering excavation. The variation of REC before and after drilling is approximately consistent with the distribution characteristics of stress and energy, which can reflect the stress concentration degree and energy accumulation level of rock mass before and after drilling in a certain degree.

In this study, only the parameter design of drilling length and drilling diameter is considered. However, under the requirements of reasonable drilling parameter design, the layout of boreholes also has a significant influence on the

prevention and control of rockburst disaster. In the next, the corresponding numerical simulation can be carried out on the parameters of drilling arrangement, such as drilling spacing and drilling number. At the same time, the selection of the optimal drilling parameters under the engineering excavation depends largely on the specific conditions of the construction site. When selecting the optimal drilling parameters, it should be closely combined with the actual site engineering, and fully consider the factors affecting the drilling pressure relief, such as geological conditions,

surrounding rock properties, excavation geometry, and construction costs.

Acknowledgements

This work was financially supported by the National Natural Science Foundation of China (52178388) and the China Postdoctoral Science Foundation Fund (2018M631114).

This is an Open Access article distributed under the terms of the Creative Commons Attribution License.



References

- [1] S. R. Wang, X. G. Wu, Y. H. Zhao, P. Hagan, and C. Cao. "Evolution characteristics of composite pressure-arch in thin bedrock of overlying strata during shallow coal mining," *In. J. Appl. Mech.*, vol. 11, no. 3, May 2019, Art. no. 1950030.
- [2] X. T. Feng, S. F. Pei, Q. Z. Jiang, Y. Yang, S. J. Li, and Z. B. Yao, "Deep fracturing of the hard rock surrounding a large underground cavern subjected to high geostress: in situ observation and mechanism analysis," *Rock Mech. Rock Eng.*, vol. 50, pp. 8, Apr. 2017.
- [3] Y. H. Zhao, S. R. Wang, Z. S. Zou, L. L. Ge, and F. Cui, "Instability characteristics of the cracked roof rock beam under shallow mining conditions," *In. J. Min. Sci. Technol.*, vol. 28, no. 3, pp. 437-444, Jun. 2018.
- [4] A. Keneti and B. A. Sainsbury, "Review of published rockburst events and their contributing factors," *Eng. Geol.*, vol. 246, pp. 361-373, Oct. 2018.
- [5] X. T. Feng, Y. X. Xiao, G. L. Feng, Z. B. Yao, B. R. Chen, C. X. Yang, and G. S. Su, "Study on the development process of rockbursts," *Chinese J. Rock Mech. Eng.*, vol. 38, no. 4, pp. 649-673, Apr. 2019.
- [6] Q. H. Qian, "Challenges faced by underground projects construction safety and countermeasures," *Chinese J. Rock Mech. Eng.*, vol. 31, no. 10, pp. 1945-1956, Oct. 2012.
- [7] A. Mazaira and P. Konicek, "Intense rockburst impacts in deep underground construction and their prevention," *Can. Geotech. J.*, vol. 52, no. 10, pp. 1426-1639, Apr. 2015.
- [8] S. R. Wang, C. Y. Li, W. F. Yan, Z. S. Zou, W. X. Chen, "Multiple indicators prediction method of rock-burst based on microseismic monitoring technology," *Arab. J. Geosci.*, vol. 10, no. 6, Mar. 2017, Art. no. 132.
- [9] C. C. Li, P. Mikula, B. Simser, B. Hebblewhite, W. Joughin, X. W. Feng, and N. W. Xu, "Discussions on rockburst and dynamic ground support in deep mines," *J. Rock Mech. Geotech.*, vol. 11, no. 5, pp. 1110-1118, May. 2019.
- [10] P. Konicek, K. Soucek, and L. Stas, "Long-hole destress blasting for rockburst control during deep underground coal mining," *Int. J. Rock Mech. Min.*, vol. 61, pp. 141-153, Feb. 2013.
- [11] F. Q. Guo, Z. C. He, and X. F. Si, "Experimental study on revealing the mechanism of rockburst prevention by drilling pressure relief: status-of-the-art and prospects," *Geomat. Nat. Haz. Risk.*, vol. 13, pp. 2442-2470, Sep. 2022.
- [12] D. Q. Liu, H. H. Liu, Y. Wang, J. Sun, M. C. He, D. Peng, and Y. F. Lan, "Experiment study on drilling pressure relief for rockburst prevention and its failure characteristics," *Chinese J. Rock Mech. Eng.*, vol. 42, no. 1, pp. 100-114, Sep. 2023.
- [13] R. E. Sousa, T. Miranda, R. L. E. Sousa, and J. Tinoco, "The use of data mining techniques in rockburst risk assessment," *Engineering*, vol. 3, no. 4, pp. 552-558, Aug. 2017.
- [14] Y. F. Wang, S. R. Wang, C. Fang, and W. Wang, "Frequency spectrum and damage characteristics of saturated and dry red sandstone subject to shear test," *Arab. J. Sci. Eng.*, vol. 48, no. 4, pp. 4609-4618, Aug. 2022.
- [15] E. Ghasemi, H. Gholizadeh, and A. C. Adoko, "Evaluation of rockburst occurrence and intensity in underground structures using decision tree approach," *Eng. Comput.*, vol. 36, no. 1, pp. 213-225, Jan. 2020.
- [16] A. A. Eremenko, S. N. Mulev, and V. A. Shtirts, "Microseismic monitoring of geodynamic phenomena in rockburst-hazardous mining conditions," *J. Min. Sci.*, vol. 58, no. 1, pp. 10-19, Jan. 2022.
- [17] A. Manouchehrian and M. Cai, "Numerical modeling of rockburst near fault zones in deep tunnels," *Tunn. Under. Sp. Tech.*, vol. 80, pp. 164-180, Oct. 2018.
- [18] X. M. Sun, M. C. He, C. Y. Liu, J. C. Gu, S. R. Wang, Z. Q. Ming, H. H. Jing, "Development of nonlinear triaxial mechanical experiment system for soft rock specimen," *Chin. J. Rock Mech. Eng.*, vol. 24, no. 16, pp. 2870-2874, Aug. 2005.
- [19] A. Manouchehrian, P. H. S. W. Kulatilake, and R. Wu, "Strainburst control in deep tunnels using a slotted excavation method," *Int. J. Geol. Mech.*, vol. 4, pp. 22, Jan. 2022.
- [20] S. R. Wang, D. J. Li, C. L. Li, C. G. Zhang, and Y. B. Zhang, "Thermal radiation characteristics of stress evolution of a circular tunnel excavation under different confining pressures," *Tunn. Under. Sp. Tech.*, vol. 78, pp. 76-83, Apr. 2018.
- [21] H. Zhao, Y. Pan, J. Lyu, Y. Peng, and S. Li, "Effect of pressure relief hole spacing on energy dissipation in coal seam at various mining depths," *Sustainability*, vol. 15, pp. 3794, Feb. 2023.
- [22] Z. F. Chen, T. Xu, C. X. Dai, and J. C. Song, "Effect of borehole positions and depth on pressure relief of cavern surrounding rock mass," *Geotech. Geol. Eng.*, vol. 40, pp. 237-248, Jun. 2021.
- [23] H. Zhang, Y. Zhu, L. Chen, W. Hu, and S. Chen, "The prevention and control mechanism of rockburst hazards and its application in the construction of a deeply buried tunnel," *Appl. Sci-basel.*, vol. 9, pp. 3629, Sep. 2019.
- [24] T. B. Zhao, W. Y. Guo, F. H. Yu, Y. L. Tan, B. Huang, and S. C. Hu, "Numerical investigation of influences of drilling arrangements on the mechanical behavior and energy evolution of coal models," *Adv. Civil Eng.*, vol. 3, pp. 1-12, Apr. 2018.
- [25] S. W. Wang, J. F. Pan, S. H. Liu, Y. X. Xia, and X. J. Gao, "Evaluation method for rockburst-preventing effects by drilling based on energy-dissipating rate," *J. China Coal Soc.*, vol. 41(S2), pp. 297-304, Dec. 2016.
- [26] C. Shi, W. J. Chu, and W. T. Zheng, *Block discrete element numerical simulation technology and engineering application*. Beijing: China Architecture and Building Press, 2016.
- [27] J. P. Li, H. X. Wang, X. G. Wang, and X. G. Cheng, "Static numerical simulation of drilling & blasting pressure relief of burst-prone rocks in tunnel wall," *J. Xi'an Univ. Archi. & Tech. (Nat. Sci. Edit.)*, vol. 47, no. 1, pp. 97-102, Feb. 2015.
- [28] H. P. Xie, Y. Ju, and L. Y. Li, "Criteria for strength and structural failure of rocks based on energy dissipation and energy release principles," *Chinese J. Rock Mech. Eng.*, vol. 17, pp. 3003-3010, Sep. 2005.
- [29] Z. H. Zhu, F. Y. Sun, and J. Q. Guo, "Study on rockburst tendency of deep underground engineering based on multi-factor influence," *Electron. J. Struct. Eng.*, vol. 23, no. 1, pp. 1-12, Jan. 2023.